Geophys. J. Int. (1991) 107, 493-503

Viability of shear-wave amplitude versus offset studies in anisotropic media

Gareth S. Yardley,[1,2] Gerhard Graham[1,2,3] and Stuart Crampin[1]

[1] *Edinburgh Anisotropy Project, British Geological Survey, Murchison House, West Mains Road, Edinburgh* EH9 3LA, *UK*
[2] *Department of Geology and Geophysics, University of Edinburgh, James Clark Maxwell Building, Edinburgh* EH9 3JZ, UK
[3] *Geological Survey of South Africa, Private Bag* X112, *Pretoria* 0001, *South Africa*

Accepted 1991 May 17. Received 1991 May 16; in original form 1991 January 16

SUMMARY

The study of shear-wave splitting can yield information about crack strike, crack density, and other parameters of the cracks and aligned inclusions within the ***in situ*** rockmass. Such information is important for reservoir characterization and other hydrocarbon production applications. Crack density is usually inferred from the percentage shear-wave anisotropy which is measured from time delays between the two split shear waves. Reservoirs may be too thin for discernible time delays to build up, and the time delay (and crack density) in a reservoir layer may be unresolvable in conventional arrival-time analysis of reflection surveys or vertical seismic profiles.

Shear-wave amplitude versus offset (AVO) techniques are studied to see if they provide a more viable method of determining anisotropic parameters in thin reservoir layers. The behaviour of reflected shear-wave amplitudes with angle of incidence is investigated in simple two-layer models. The variations in shear-wave AVO are calculated for a range of percentage shear-wave anisotropies for water-filled cracks and dry cracks in the second layer (representing a reservoir) to see if characteristic information about reservoir properties can be extracted from the shear-wave AVO signatures. The shear-wave AVO curves, for thin cracks, are sensitive to changes in anisotropy and crack content. Most of the information about crack content is contained in wide offset reflection data which suggests applications in crosshole monitoring of enhanced oil recovery. The variations in shear-wave AVO may be distorted by the acquisition system. Most of the information about the percentage anisotropy is contained in the amplitudes of shear waves reflected at near-vertical angles of incidence. Vertical incidence reflection amplitude methods are reviewed and a simple graphical procedure is suggested for determining their viability in different reservoir environments.

Key words: anisotropy, fractured reservoirs, shear-wave AVO , shear-wave splitting.

1 INTRODUCTION

Upon entering an anisotropic medium, a shear wave splits into (usually) two approximately orthogonal components. For nearly vertical ray paths, the polarization direction of the faster shear wave is usually parallel to the strike of the typically parallel vertical cracks within the rockmass (Crampin 1987). The delay between the two shear-wave components is a function of the percentage anisotropy along the particular ray path. Hence, it has been suggested (Crampin, Lynn & Booth 1989) that the split shear waves contain information about the preferential directions of fluid flow within a hydrocarbon reservoir and the crack density of the reservoir rock. Consequently, it may be possible to locate highly fractured reservoirs by analysing shear-wave splitting, and estimate the valuable parameters of crack density and direction of fluid flow within a reservoir.

It is usually necessary for observable delays to build up between the fast and slow shear-wave arrivals before the direction of polarization of the shear wave can be determined by analysing transmitted or reflected shear waves directly. Many reservoirs are too thin for sufficient

time delays to build up. In many cases, such as the Austin Chalk in Texas, where the structure is uniform nearly horizontal plane layers, it is likely that the crack orientation will be constant throughout the whole depth range, and the azimuth of anisotropy determined for the whole section will be that of the reservoir. Alford (1986) showed reflection sections from Dilley, Texas where the delay between the fast and slow sections increases with depth indicating that the azimuth of anisotropy, and by inference the crack strike, remains constant with depth. However, even in such cases information about the crack density in the reservoir layer will be hard to resolve. It has therefore been suggested (Thomsen 1988) that the analysis of reflected amplitudes from anisotropic reservoirs may resolve this difficulty as the reflection coefficient parallel to the cracks will be different from that perpendicular to the cracks.

Ostrander (1984) showed how the study of amplitude variations with offset for reflected P-wave data could be used to distinguish between seismic bright spots caused by the presence of gas sands and those due to other phenomena, such as dense intrusions with high seismic velocities. In studies of P-wave amplitude versus offset (AVO), information about the change in Poisson's ratio at a reflector is seen in the behaviour of the reflected P-wave amplitude with offset. The aim of this paper is to see whether reflected shear-wave amplitudes also contain characteristic information about the reflecting reservoir layer, particularly in the presence of anisotropy. We investigate the reflected shear-wave amplitude variations with offset (shear-wave AVO), over a range of reservoir properties, to see if this holds characteristic information. Previous work on vertical incidence reflections is reviewed, and an attempt is made to quantify their range of applications.

In this paper, synthetic seismograms have been calculated using a full-waveform modelling package (Taylor 1990), and used to model effectively anisotropic solids containing distributions of aligned cracks, derived from the formulations of Hudson (1980, 1981). All anisotropic models described are modelled as media with hexagonal symmetry and with horizontal axes of symmetry, consistent with the presence of vertical stress-aligned cracks, microcracks, and preferentially oriented pores in the rockmass. The velocity structures used are typical (but non-specific) of rocks in sedimentary basins. A Poisson's ratio of 0.25 is used throughout which gives a V_P/V_S ratio of 1.73. Note that the use of terminology *SV-* and SH-waves is only appropriate in wholly isotropic layers. In anisotropic layers shear waves are referred to as the faster and slower split shear waves, $S1$ and $S2$ respectively.

2 SHEAR-WAVE AVO

In this section, we investigate the amplitude variation with offset of reflected shear waves, and seek evidence of characteristic information about the reservoir structure. To investigate the characteristics of shear-wave reflection, we look at reflections from the interface in a range of simple two-layer models, the second layer representing the cracked or fractured reservoir layer. For each set of models, the properties of the upper layer remain fixed whilst the properties of the lower (reservoir) layer are varied. The graphs of reflection coefficients against angle of incidence at an isotropic/anisotropic interface were calculated using a program adapted from the work of Booth & Crampin (1983). Booth & Crampin (1983) generalized the reflectivity technique of Fuchs & Müller (1971) to cope with anisotropic media in a program for calculating synthetic seismograms. The reflectivity technique makes use of propagator matrices (Gilbert & Backus 1966) to describe plane wave motion in a sequence of plane horizontal layers. A formulation for the calculation of propagator matrices for anisotropic structures was developed by Crampin (1970). Graphs of reflection coefficient against incidence angle at an isotropic/isotropic interface were calculated using modified Zoeppritz's equations (McCamy, Meyer & Smith 1962; Aki & Richards 1980).

[Note that the technique of Booth & Crampin (1983) does not take account of azimuthal variations. Thus, the calculations are only strictly correct for propagation in planes of sagittal symmetry, although for non-sagittal symmetry the differences are likely to be negligible for weak anisotropy.]

In studying shear-wave AVOs, we are looking for characteristic differences in the shape of the variation of the reflection coefficients with the angle of incidence for varying properties of the reservoir. A fractured reservoir might be identified by comparing the variation of the AVO curves along a shear-wave reflection line, and locating the reservoir characteristics from their signature in the AVO curves. We examine how reservoir anisotropy and pore-fluid content affect the shear-wave AVO response.

2.1 Sensitivity to anisotropy and fluid content

In anisotropic media, the shear-wave velocity generally varies with angle of incidence and azimuth. It is therefore expected that the variation of the reflection coefficient against angle of incidence at an isotropic/anisotropic interface will change with azimuth and with the percentage anisotropy in the reflecting layer. The change in shape of the shear-wave AVO curve with anisotropy is expected to yield information about the percentage of anisotropy in the reflecting (reservoir) layer.

Fluids cannot support shear stresses (King 1966) and it might be supposed that changing the content of the fluid in cracks would have no effect on the shear-wave reflectivity. However, if the fluid is contained in thin pores or cracks then shear waves propagating at an angle to the surface of the inclusions will exert some compressional force on the fluid within the cracks. For vertical propagation, the shear-wave velocity is principally dependent on the rock matrix properties, but for all other directions, except strictly horizontal, the behaviour of shear waves is modified by vertical cracks. In addition, because the two split shear waves will behave differently at the surface of the inclusions, even small differences between the shear waves are likely to lead to identifiable changes in the highly sensitive polarization diagrams (hodograms) of the particle displacements.

[The situation for P-wave AVOs (Ostrander 1984) is more dramatic. Liquids and gases have greatly different compressibilities and therefore different P-wave velocities: at 40 °C, heavy crude oil has a P-wave velocity of about

1.4 km s^{-1} (Wang & Nur 1988), whereas methane has a P-wave velocity of 0.47 km s^{-1} (Kaye & Laby 1986). With increasing incidence angle at a reflector at a water-saturated sand more ***P-wave*** energy is mode converted to refracted and reflected shear waves giving rise to a decrease in reflected P-wave energy with offset. As the sediment becomes partially saturated with gas the P-wave velocity decreases quickly due to the change in compressibility caused by the presence of gas in the pores (the greatest decrease in P-wave velocity occurs over the first 3 to 8 per cent of gas saturation). This reduction in the P-wave velocity can cause an increase in P-wave reflectivity (at, for example a gas sand to shale interface), without substantially affecting the shear-wave reflectivity (for angles of incidence out to about 40°, as will be shown later in this section). This means that a larger proportion of the incident P-wave energy goes into reflected compressional waves and can lead to an increase in reflected P-wave amplitude with offset.]

Figure 1 shows the variation of reflection coefficient with angle of incidence for SV-waves at an isotropic/anisotropic reflector. The second layer represents a possible reservoir in which the differential shear-wave velocity anisotropy varies from 0 to 20 per cent. The anisotropy is assumed to be caused by parallel vertical cracks with a range of crack densities aligned normal to the plane of incidence. The coefficients are shown for both dry (gas-filled) and water-filled cracks to illustrate the range of possible variations in rock properties due to crack content. The upper layer is isotropic for simplicity. Thin cracks with an aspect ratio of 0.01 are used. Similar graphs were calculated for a range of velocity contrasts from a velocity increase of 15 per cent, to a velocity decrease of 15 per cent, across the interface, however, the general results are the same as described here. The cracks were modelled by the formulations of Hudson (1980, 1981) as adapted by Crampin (1984).

Figure 1 shows that for both water-filled and dry cracks the amplitude of the near-vertical reflected wave increases with percentage anisotropy in the reservoir layer. The cracks, in this case, are in the cross-line direction and the SV-wave is polarized parallel to the slow direction in the lower layer. For thin cracks, the formulations of Hudson (1980, 1981) indicate that the velocity parallel to the cracks does not change appreciably with anisotropy, however, the velocity perpendicular to the cracks decreases with increasing anisotropy giving rise to a larger velocity contrast (at a high-to-low velocity interface) for a wave polarized perpendicular to the cracks and an increase in the near-vertical reflection coefficient with increasing anisotropy for the ***SV-wave.*** It can also be seen that the critical angle (the zero point) of the curves increases by about 6” as anisotropy is increased from 0 to 20 per cent.

There is a large difference in the shape of the AVO curves for wide offsets between the water-filled and dry cracks, but little change in critical angle. This is because, for thin cracks, the shear-wave line singularity moves away from the vertical as the content of the cracks changes from water-filled to gas-filled. In many cases cracks or fractures are likely to be thin (Corbett, Friedman & Spang 1987). The results here extend to the monitoring of enhanced oil recovery in which the fluid content of the reservoir is changed by either heating the fluid or injecting further

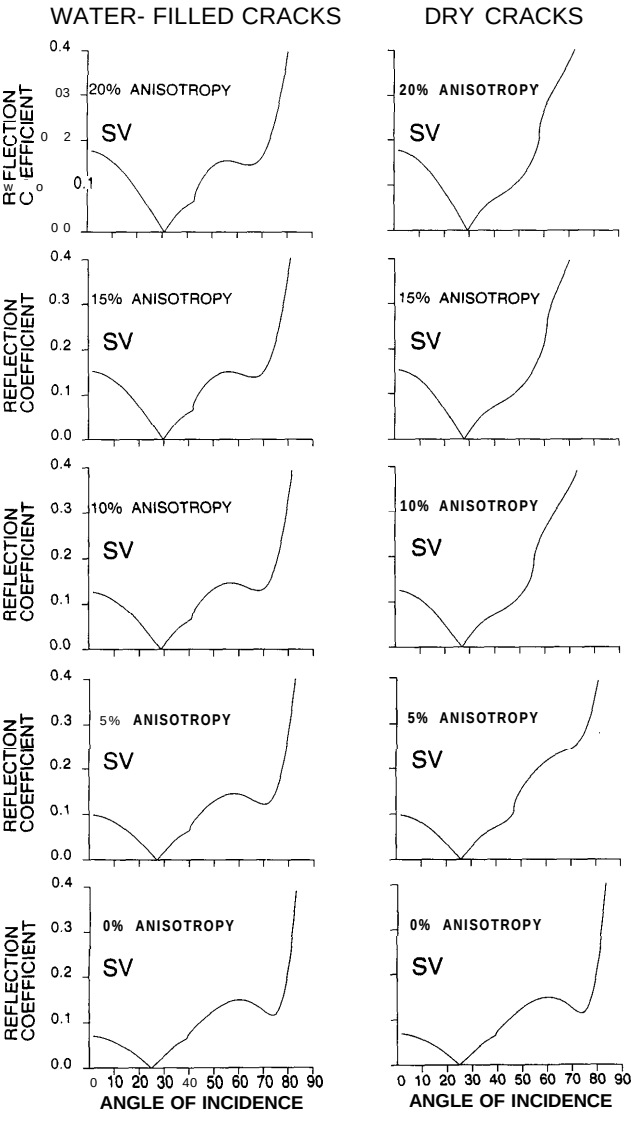

Figure 1. Plots of reflection coefficients against angle of incidence at an isotropic/anisotropic interface for SV-waves for a range of differential shear-wave anisotropies at a high-to-low velocity interface (matrix density, V_P and V_S are 2.3 g cm^{-3}, 4.76 and 2.75 km s^{-1} in Layer 1, and 2.2 g cm^{-3}, 4.33 and 2.5 km s^{-1} in Layer 2, respectively). The anisotropy is modelled by parallel vertical cracks aligned normal to the plane of incidence. Graphs are shown for both water-filled and dry (gas-filled) cracks. For thin cracks, percentage anisotropy is equal to crack density multiplied by 100.

fluids. The changes in the rock matrix velocities due to heating are small (Wang & Nur 1988) and will not greatly affect the shear-wave reflectivity. Shear-wave reflectivity may be affected by the viscosity of the liquid in the cracks, however, the difference in shear-wave velocity between sandstones saturated with water (low viscosity) and heavy crude (high viscosity) is small (Wang & Nur 1990). [The probably more significant differences in shear-wave attenuation between low- and high-viscosity fluids have not yet been fully investigated, and could lead to considerable differences in the differential amplitudes of split shear waves in cracked structures.]

The large changes in the shape of the shear-wave AVO

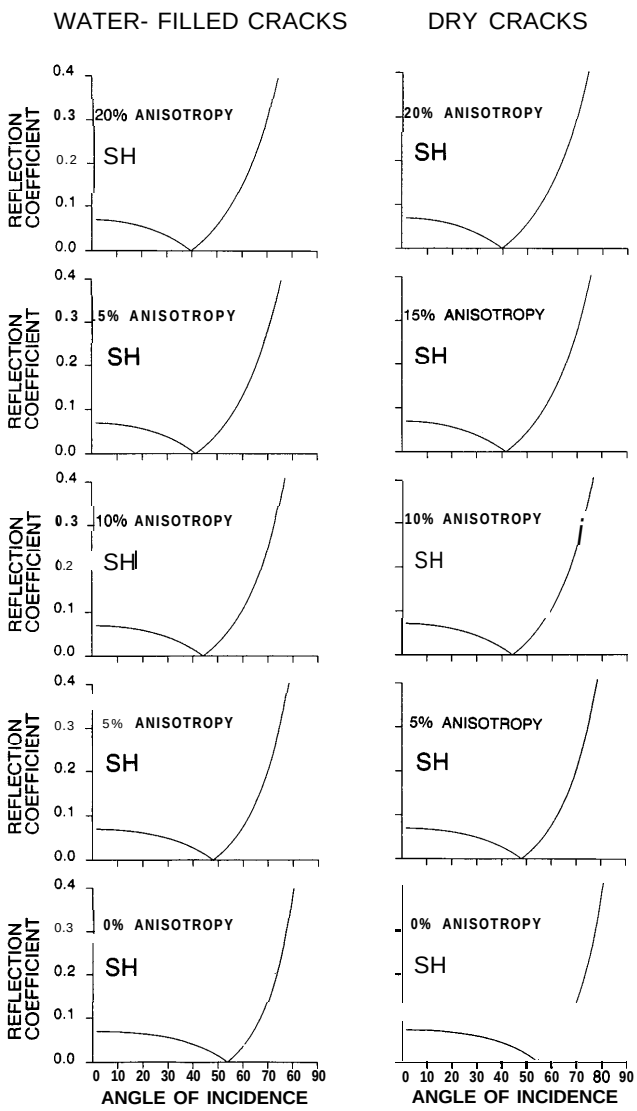

Figure 2. Plots of reflection coefficients against angle of incidence at an isotropic/anisotropic interface for W-waves for the same range of models used in Fig. 1.

curves occur at isotropic/anisotropic reflectors for angles of incidence greater than about 40". There are more subtle changes in differential behaviour between ***SV***- and SH-waves for angles of incidence greater than about 20°, which could lead to significant differences in the polarization diagrams. These angles of 40" and 20" may be too wide to be observed in most reflection profiles, unless the reflector is shallow. However, changes in the amplitude of the reflected shear-wave signal with crack content should be visible in shear-wave monitoring of enhanced oil recovery in a crosshole surveys.

In Fig. 2 similar reflection coefficient against angle of incidence graphs are plotted for the SH-wave. There is no change in the vertical incidence reflection coefficient, as the wave is polarized parallel to the cracks and, for thin cracks, is not affected by changing anisotropy. The position of the zero point changes by about 15" as the percentage anisotropy is increased from 0 to 20 per cent. This is caused by the change in shear-wave velocity with incidence angle in an anisotropic medium. There is no difference in the reflection coefficients for water-filled and dry cracks as the SH-wave does not generate any compressional forces in the thin cracks. [Note that the differences in the behaviour of ***SV***- and SH-waves on reflection would lead to very significant differences in the polarization diagrams of the reflected waves from incident shear waves with polarizations intermediate to ***SV*** and ***SH.]***

In the above discussion, the cracks were aligned in the cross-line direction. For cracks orientated in the in-line direction (not shown here) the shear wave velocities in the anisotropic layer do not vary with offset and so the position of the zero points do not change with anisotropy. Also for in-line thin cracks there is no difference between the shear wave AVO curves for water-filled and dry cracks. However, there is a change in the near-normal reflection coefficient for the SH-wave, which would be polarized perpendicular to the cracks. For a general orientation of the cracks with respect to the acquisition line there will be variations in shear-wave AVO for both percentage anisotropy and crack content for thin cracks. As cracks are made wider the observed change in shear-wave AVO with crack content decreases until there is no change for spherical pores. As the number of cracks is increased, there is a change in the near-vertical reflection coefficients as the shear-wave velocity of the medium decreases due to the reduction in matrix material and this may also provide means of distinguishing between areas with low and high crack densities within a reflector.

Thus, it can be seen that the largest change in the shear-wave AVO curves is in the near-normal reflection coefficients. A comparison of the near-normal incidence reflected amplitudes for the shear waves polarized parallel and perpendicular to the fractures will yield information about the percentage anisotropy caused by parallel, vertical cracks in the reflecting layer. The variation of vertical incidence amplitudes has been studied by Spencer & Chi (1990) and used in the field by Mueller (1991, this issue) and will be discussed in Section 3, below.

The reflected amplitudes of shear waves are more difficult to interpret if the cracks in the reflecting layer are not aligned parallel to the in-line or cross-line directions as the shear-wave polarizations will be rotated on reflection. This is because the reflecting layer will have different reflection coefficients parallel and perpendicular to the crack strike. In this case, where the upper layer is isotropic, both the incident ***SV***- and SH-waves will be rotated upon reflection. At a low-to-high velocity interface the incident shear waves would rotate towards the crack strike (and away from the crack strike for a high-to-low velocity interface) and would not have ***SV*** and ***SH*** polarizations after reflection. The reflected shear waves (one from the in-line and one from the cross-line source) would have the same two-way traveltime and would not be perpendicular to each other after reflection. This means that even for near-normal reflections a source-geophone rotation (Alford 1986) would not be able to resolve the crack strike in the reflecting layer. It must be noted that the source-geophone rotation was not designed for dealing with such data, but rather for split shear waves which have travelled for a large part of their path length through anisotropic media with near-vertical ray paths. The situation is even more complex with offset

arrivals where the polarization of the fast split shear wave in the anisotropic layer need not be parallel to the crack strike.

In the above section it has been shown that changes in anisotropy and fluid content in the reflecting layer lead to changes in the shear wave AVO curves. To study shear-wave AVOs with field data, it is desirable to have near noise-free and distortion-free data. We conclude that shear-wave amplitudes may be difficult to measure for reflections from an isotropic/anisotropic interface if the cracks in the lower layer are not parallel or perpendicular to the in-line direction. Further distortions are likely if the upper layer is anisotropic.

2.2 Modelliug field measurement of shear-wave AVOs

Liu, Crampin & Yardley (1990) described the distorting effects on reflections for an isotropic/isotropic interface if the source polarization was not strictly ***SV*** or ***SH.*** The distortions are caused by the difference in behaviour of the reflection coefficients with offset for ***SV***- and SH-waves leading to an effective rotation of the shear-wave signal. Such distorting effects would also be seen for vertical incidence at a dipping reflector. In general, shear-wave reflection surveys in the field use in-line and cross-line source orientations. In such cases, it might be thought that the effects described by Liu et al. (1990) would be of no concern as shear waves with polarizations parallel and perpendicular to the in-line direction are generated at the source. However, if the strike of the cracks in the upper layer is not in the acquisition plane, the shear waves split on their way to the reflector. The shear waves generated at the source split into two components which are polarized parallel and perpendicular to the crack strike, and are distorted at the reflector. This leads to distortions in the measured shear-wave amplitudes. Both of the downward-travelling shear waves then undergo an effective rotation upon reflection at the interface (Liu et al. 1990) and will be split again on their upward path. This means that for a non-normal reflection, no matter what the source orientation, both the fast and slow shear-wave polarizations would be excited. A source-geophone rotation (Alford 1986) would not recover the required shear-wave amplitudes. These results also apply to shear waves generated by mode conversions from P-waves (at the sea floor in a marine VSP, for example), which are reflected at a deeper interface. In Figs 3, 4, 5 and 6, below, these relative distortions are examined in more detail.

In the preceding discussion, shear-wave AVOs were examined for a model with an upper layer, which for simplicity was isotropic. Now we will discuss the distorting effects caused by an anisotropic upper layer. Field observations show that there is probably more anisotropy in the near-surface than at deeper levels (Bush 1990; Becker et al. 1990). In this case the second layer has been kept isotropic so that only the distortions due to the presence of the upper layer are seen. Cracks have been inserted in the upper layer with an aspect ratio of 0.01 and a crack density of 0.05 to give a differential shear-wave velocity anisotropy of approximately 5 per cent.

Figure 3 shows the acquisition geometry for two reflection lines in the same model structure. In **Fig. 3(a),** the cracks are parallel to the in-line direction, whereas in **Fig.** 3(b), the

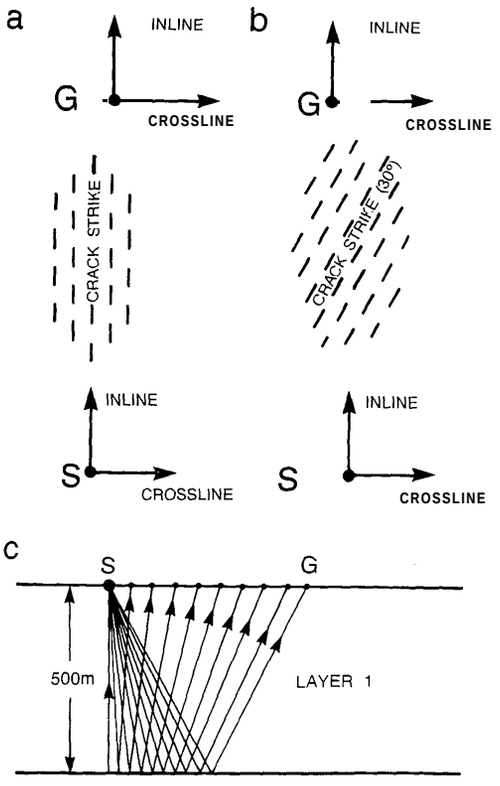

Figure 3. Schematic diagrams showing the plan view of acquisition geometry for a simple reflection line for two cases: (a) crack strike parallel to the acquisition plane; and (b) crack strike 30° from the acquisition plane. In these models the upper layer is anisotropic and the lower reflecting layer is isotropic. (c) Section of acquisition geometry. S marks the source location and there are 10 geophones 60 m apart. Incidence angles range from 0° to 28" and are within the she&-wave window. Matrix density, V_P and V_S are 2.3 g cm^{-3}, 4.33 and 2.5 km s^{-1}, and 2.2 g cm^{-3}, 4.07 and 2.375 km s^{-1} in Layers 1 and 2 respectively.

crack strike is 30" from the in-line direction. Fig. 3(c) shows a side view of the acquisition geometry. Incidence angles range from 0" to about 28" and are within the shear-wave window (Booth & Crampin 1985). In Fig. 4, the horizontal plane polarization diagrams are plotted windowed around the reflected shear-wave arrival for both the models. Fig. 4(a) shows that shear-wave arrivals are linear from a source which is polarized either parallel or perpendicular to the crack strike. It would be possible to measure the amplitudes of such arrivals after the usual AVO corrections for spherical divergence and NMO, etc. (Ostrander 1984). Fig. 4(b) shows that the arrivals from a model in which the cracks are 30" to the in-line direction have been distorted, and without detailed knowledge of the anisotropic structure and the initial pulse shape it would not be possible to estimate the undistorted shear-wave amplitude. The polarization diagrams shown in Figs 4(a) and (b) are fundamentally different from each other, and the information shown in Fig. 4(a) cannot be recovered from Fig. 4(b) by a simple source-geophone rotation, because of the effects described by Liu et ***al.*** (1990).

Figure 5 shows the polarization diagrams after the model has been recalculated with the sources and geophone axes

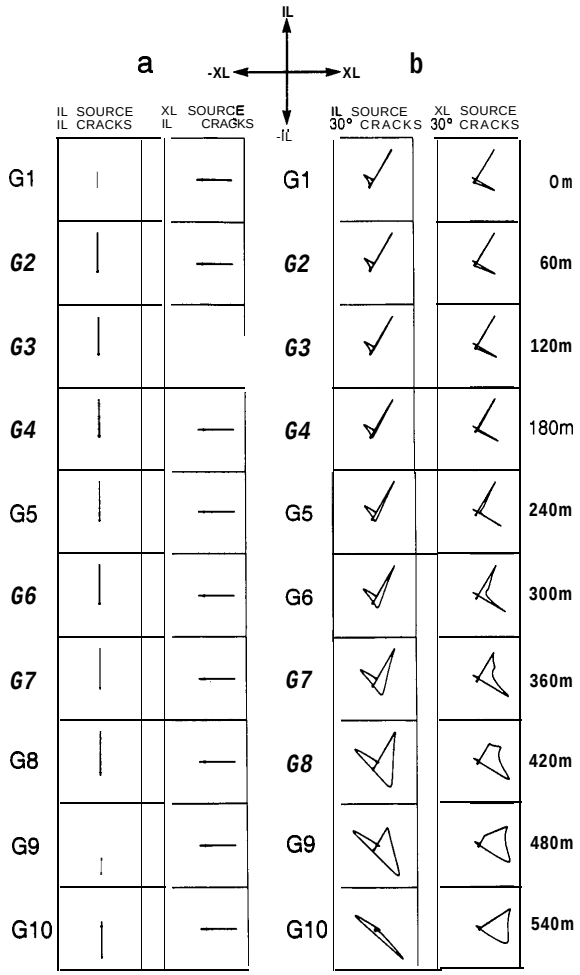

Figure 4. Horizontal plane polarization diagrams around the reflected shear-wave arrival normalized within each box for the model shown in Fig. 3. In-line (IL) and cross-line (XL) directions indicated. The polarization diagrams in (a) with crack strike parallel to the acquisition plane show linear motion. The polarization diagrams in (b) are non-linear due to the source wavelet being split by the anisotropic medium. In this case, direct amplitude information may be severely disturbed.

parallel and perpendicular to the crack direction. For near-vertical angles of incidence this is equivalent to a source-geophone rotation (Alford 1986). The source parallel to the cracks only excites the downgoing fast shear wave and the source perpendicular to the cracks only excites the downgoing slow shear wave. The incident shear waves do not arrive at the reflector with polarizations either parallel or perpendicular to the in-line direction, and for non-normal angles of incidence the reflected shear waves are distorted. Such distortions are seen in Fig. 5(b), where the polarization diagrams change from linear for near-vertical incidence reflections (geophones 1 to 3, incidence angles of 0" to 7") to progressively more distorted shapes (geophones 4 to 10, incidence angles of 10" to 28"). This shows that to preserve the shape of the shear-wave AVO curves in the presence of near-surface anisotropy it is necessary for the acquisition plane to be parallel or perpendicular to the crack strike, that is the acquisition plane must be in a symmetry plane. We have commented earlier that if the acquisition plane is parallel to the cracks it will not yield any shear-wave AVO information as the shear-wave velocities do not change with angle of incidence for this azimuth. This means that the acquisition plane must be perpendicular to the cracks to be able to record any changes in shear-wave AVO with increasing crack-induced anisotropy without encountering such distortions in the shear-wave amplitudes.

It may be possible with accurate information about the source pulse and velocity structure of the overlying layers to strip off the effects of these distortions. This may be desirable as then information about the shear-wave AVOs both perpendicular and parallel to the cracks would come from a single source. Where two sources are used to investigate reflected amplitudes the relative energy generated by each source must be known. However, at present our knowledge of source pulse shapes may not be adequate (Ziolkowski 1991).

Such distortions as described by Liu et al. (1990) occur at angles of incidence where ***SV*** and ***SH*** reflection coefficients become different. In Fig. 6, we show where such anomalies occur for a range of interface parameters. Fig. 6 shows the

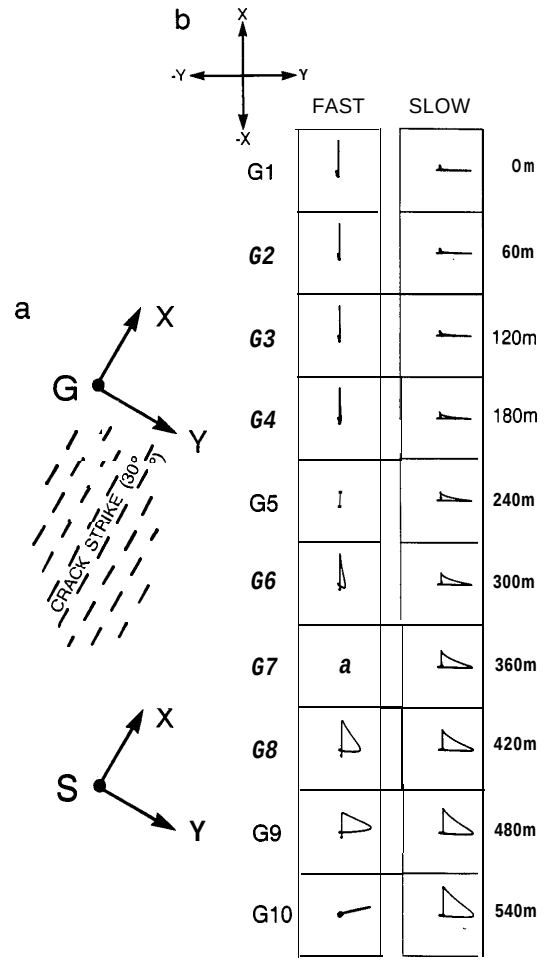

Figure 5. Seismograms from Fig. 4(b) have been recalculated for the source parallel to and perpendicular to the crack strike. The horizontal polarization diagrams show that the recorded shear-wave arrival is non-linear for offsets of greater than a few degrees. The X direction is parallel to the strike of the cracks.

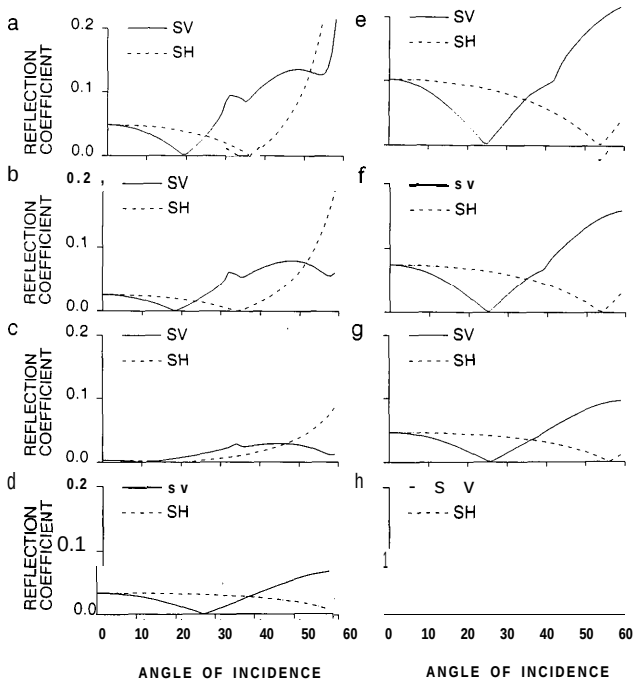

Figure 6. Reflection coefficients for ***SV***- and W-waves against angle of incidence for a range of velocity contrasts. The reflection coefficients for the ***SV***- and W-waves diverge for incidence angles of only a few degrees from the vertical. This leads to distortions in the reflected shear-wave if the incident wave was not strictly polarized ***SV*** or ***SH***. Model parameters are given in Table 1.

variation of reflection coefficients with offset for ***SV***- and SH-waves for an isotropic/isotropic interface for a range of velocity contrasts from low-to-high to high-to-low. An isotropic/isotropic interface is used for simplicity so that such distortions are not confused with the added effects caused by the presence of anisotropy. The model parameters are shown in Table 1.

Figure 6 shows that in most cases the ***SV*** and ***SH*** reflection coefficients deviate from each other at incidence angles more than a few degrees. Exceptions to this are in Figs 6(c) and (d), where both reflection coefficients are small for near-vertical incidence. In the models in Table 1, the density of Layer 2 was held constant so that the observed

Table 1. Parameters used in calculating the reflection coefficient against angle of incidence graphs shown in Fig. 6.

		Density (g/cm³)	*Vp* (km/s)	*Vs* (km/s)
Layer 1		2.3	4.33	2.50
Layer 2	a	2.2	4.98	2.88
	b	2.2	4.76	2.75
	c	2.2	4.55	2.63
	d	2.2	4.42	2.55
	e	2.2	4.24	2.45
	f	2.2	4.07	2.38
	g	2.2	3.90	2.25
	h	2.2	3.68	2.13

effects are only due to changes in velocity contrast. Changes in density contrast will also affect the amplitude of the reflected waves. In all cases,. the ***SV*** and ***SH*** curves diverge for angles of incidence greater than about 12°, and in most cases for smaller angles of incidence. Fig. 6(f) has the same isotropic parameters as used for the models in Figs 3, 4, and 5. It can be seen in Fig. 5(b) that the difference in ***SV*** and ***SH*** reflection coefficients starts at about 4". This causes noticeable distortions at about geophone 4 (angle of incidence 10"). There are slight differences between Figs 5(b) and 6(f) as Fig. 6 has been plotted for an isotropic/isotropic interface for simplicity. Such distortions are likely to cause problems in CMP stacking of reflection data as the waveforms will become increasingly distorted with offset. However, in many cases, the reflectors of interest are deep, and all the reflected traces to be stacked have incidence angles within a few degrees of normal incidence. For such near-normal angles of incidence distortions are small.

3 SHEAR-WAVE REFLECTIONS AT VERTICAL INCIDENCE

Shear-wave AVOs give information about the percentage anisotropy in a reflecting layer. However, problems associated with anisotropic near-surface layers mean that it is difficult to measure the amplitudes of the offset shear-wave arrivals. Crack density is of direct relevance to the hydrocarbon industry, and a comparison of the vertical incidence amplitudes of the reflected fast and slow shear waves may yield information about the anisotropy and hence crack density in the reflecting layer. Such a comparison forms the basis of theoretical work by Spencer & Chi (1990) and analysis of field data by Mueller (1991).

If a linearly polarized shear wave is reflected from an isotropic/anisotropic interface, where the cracks in the lower layer are not aligned parallel to the polarization of that wave, the wave will change polarization upon reflection. This is because the reflection coefficients are different for the components of the wave parallel and perpendicular to the crack strike. The amount by which the wave changes polarization will depend on the strength of anisotropy in the lower layer, the velocity contrast, and the difference between the shear-wave polarization and the crack strike.

Spencer & Chi (1990) extended this principle to looking at very thin reservoir layers where the reflections from the top and bottom of the reservoir interfere. The resulting shear-wave arrival is an ellipse where the direction of the major axis of the ellipse indicates the percentage anisotropy in the reservoir layer for cases where the initial source was not polarized either parallel or perpendicular to the cracks in the reservoir. With increasing anisotropy, the direction of the major axis of the ellipse for the reflected shear wave increasingly deviates from the original source direction. This approach is demonstrated in Figs 7(a)-(c), which shows horizontal plane polarization diagrams windowed about the reflected shear-wave arrival for vertical incidence. The source is a horizontal shear-wave source polarized in the Y direction. The model consists of a 20 m thick reservoir layer (density = 2.4 g cm^{-3}, $V_P = 4.33$ km s^{-1}, $V_S = 2.5$ km s^{-1}) sandwiched between two 1 km layers of rock (density =

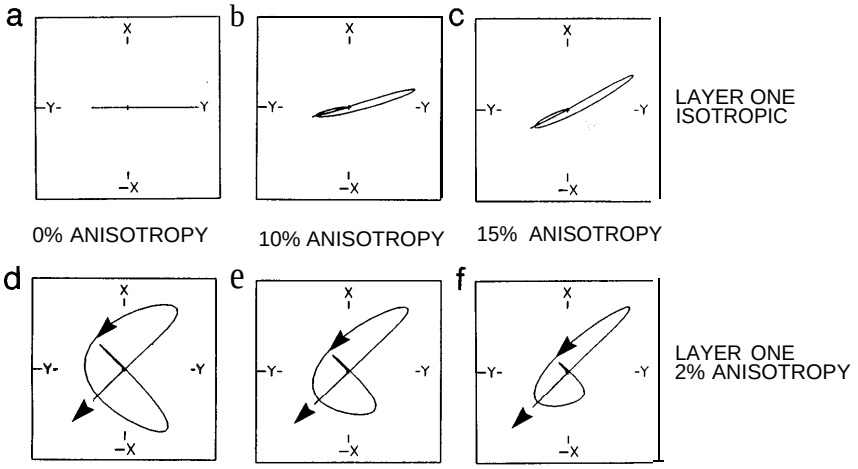

Figure 7. Horizontal polarization diagrams of the reflected shear-wave signals for a vertical incidence reflection from a thin reservoir layer for increasing reservoir anisotropy. Two cases are shown: (a), (b), (c) upper layer is isotropic, and the direction of the major axis of the shear-wave ellipse progressively rotates away from the source orientation and towards the crack strike as the reservoir anisotropy is increased; and (d), (e), (f) upper layer is anisotropic, and first motions (marked by arrows) of the shear waves are now determined by the fracture strike direction in the upper layer. The source is polarized in the Y direction and all cracks strike at **X45°Y**. See text for model parameters.

$2.4\ \mathrm{g\,cm^{-3}}$, $V_P = 3.46\ \mathrm{km\,s^{-1}}$, $V_S = 2.0\ \mathrm{km\,s^{-1}}$). The source pulse used has a dominant frequency of 25 Hz.

In each of the anisotropic layers (see Fig. 7) the cracks strike at **X45°Y**. It can be seen that the direction of the major axis of the elliptical motion deviates progressively from the source polarization as the percentage anisotropy in the reservoir layer is increased. This technique is critically dependent on the velocity contrast at the top and bottom of the reservoir layer, and effects may vary widely with different matrix parameters in the three layers, and also with the thickness of the reservoir layer with respect to the seismic wavelength.

The technique of Spencer & Chi (1990) along with all techniques which look for rotation of the reflected shear wave signal with respect to the original source polarization, is likely to be unusable when applied to field data, because the overburden is also likely to be anisotropic. Figs 7(d)-(f) show the results if the previous models are repeated but with 2 per cent anisotropy in the upper layer, with cracks striking in the same direction as the cracks in the reservoir layer. It can be seen that the direction of the first arrivals are now fixed by the anisotropy in the upper layer. The change in anisotropy of the reservoir layer changes the relative energy in the interference lobes between the split shear waves. Such a difference is hard to interpret quantitatively in terms of anisotropy in the reservoir layer and may be hidden by noise in field data or lateral inhomogeneities (for this technique to work the reflected shear-wave signal from one site must be compared with others to check for anisotropic reservoir regions). It may be possible to employ a layer stripping technique to remove the effects of near-surface anisotropic layers. However, such techniques are likely to increase errors in the determination of the anisotropic parameters. Below, we review an alternative method of using reflected amplitudes, which does not require a layer stripping approach.

Mueller (1991) presented a simple way of comparing the fast and slow reflection coefficients for entire shear-wave reflection sections from the Austin Chalk, Texas, where the production is largely controlled by fractures in the chalk. The field data were processed and rotated into fast (polarized parallel to the fractures) and slow (polarized perpendicular to the fractures) sections. An increase in anisotropy (at a reservoir) in part of a given layer will reduce the shear-wave velocity of that layer perpendicular to the factures but the velocity parallel to the fractures will remain unchanged (for thin fractures). For cases where the reservoir layer has a velocity a few per cent higher than the overlying rock this will cause the amplitude of the reflection on the slow shear-wave section to be reduced. This is due to the decrease in the reflection coefficients perpendicular to the cracks in the reservoir region.

The principles behind this are demonstrated in Figs 8 and 9. Fig. 8 shows the multilayered model with parameters in Table 2. Fig. 9 shows synthetic seismograms for source and geophone polarizations parallel and perpendicular to the aligned fractures. The shear-wave velocities used in the model are consistent with a simplified structure from the Austin Chalk, Texas. The fractured reservoir is clearly seen as the region in which the reflection amplitudes from the top of layers three and four are reduced in section perpendicular to the cracks. In Figs 8 and 9 Layer 3 is shown with a central reservoir section in which there is a 15 per cent differential shear-wave velocity anisotropy. This was achieved by combining data from two models; one with an isotropic Layer 3; one with an anisotropic Layer 3. This technique has been used successfully to locate fractured reservoirs in the Austin Chalk in Texas by Mueller (1991) who looked for and found reflection discontinuities in the slow shear-wave section, as shown in Fig. 9. The location of the fractures was subsequently confirmed by horizontal drilling.

For this technique to work successfully a number of conditions must be met. The percentage anisotropy in the reservoir layer and the velocity and density contrasts must be such that the reflection coefficient parallel to the fractures is measurably different from that perpendicular to the

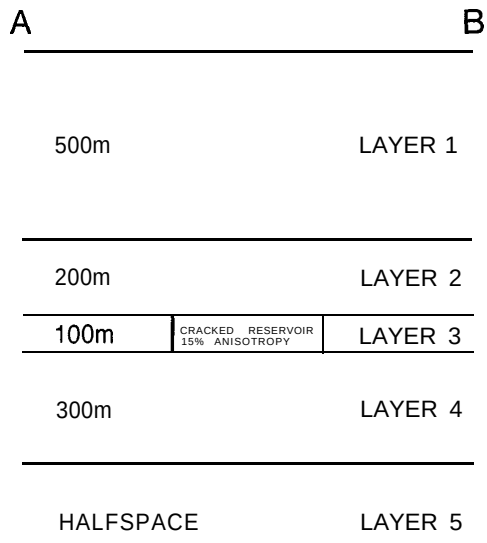

Figure 8. Schematic model of a multilayered earth containing a region with 15 per cent shear-wave velocity anisotropy in Layer 3 simulating a fractured reservoir. The model parameters are in Table 2.

Table 2. Parameters used in the model shown in Figs 8 and 9. All the layers are isotropic except for Layer 3(b) which was made , by inserting thin vertical cracks into Layer 3(a) to give a 15 per cent shear-wave anisotropy. The crack strike is perpendicular to the model section.

	Density (g/cm^3)	Vp (km/s)	Vs (km/s)
Layer I	2.1	3.00	1.70
Layer 2	2.2	3.46	2.00
Layer 3a	2.2	4.33	2.50
Layer 4	2.2	3.46	2.00
Layer 5	2.5	5.00	2.88

		$S1$ (km/s)	$S2$ (km/s)
Layer 3b	2.2	4.33	2.50 2.125

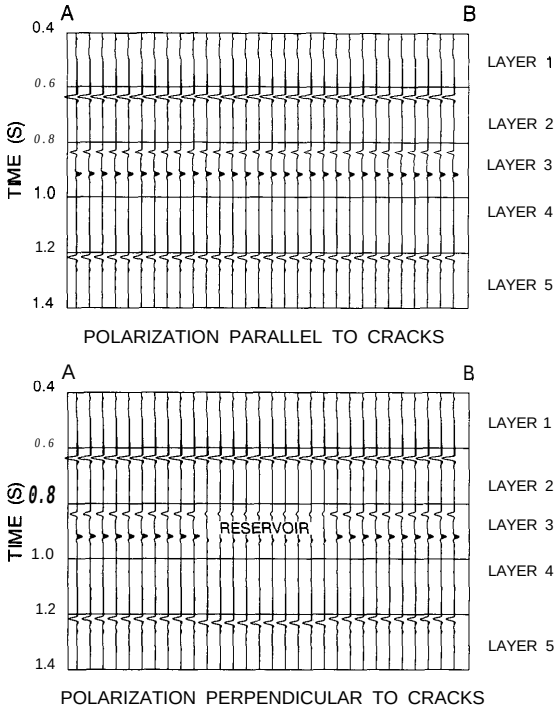

Figure 9. Synthetic shear-wave normal incidence sections for the model shown in Fig. 8 for source polarizations parallel and perpendicular to the fracture direction. The reflections from the top of Layer 3 and the top of Layer 4 are continuous for the fast shear-wave section (source parallel to cracks) but discontinuous for the reservoir region for the slow shear-wave section (source perpendicular to cracks). The reflection from the top of Layer 5 has undergone a velocity pull-down in the slow section; the size of the pull-down is dependent on the thickness and anisotropy of the reservoir layer. The dominant frequency of the source pulse is 25 Hz.

fractures and the reflection coefficients must not be negligibly small. We examine the range of circumstances over which such investigations of the vertical incidence reflection coefficient could provide useful results. Fig. 10 shows the vertical incidence reflection coefficients at an isotropic/anisotropic interface for a range of velocity contrasts and a range of anisotropies for the shear wave polarized perpendicular to the crack strike. The matrix

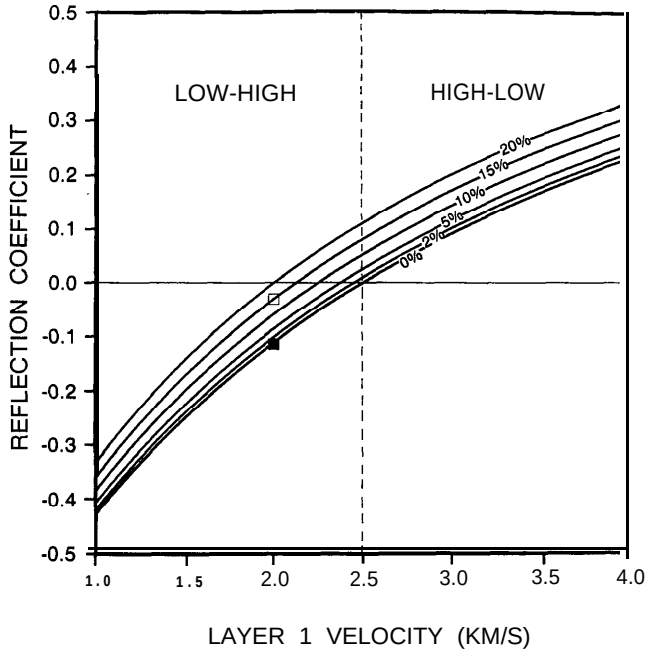

Figure 10. Vertical incidence reflection coefficients for reflection at a simple isotropic/anisotropic interface for the source polarized perpendicular to the cracks (slow shear wave) for a range of anisotropy percentages and a range of shear-wave velocity contrasts. The shear-wave velocity of Layer 1 varies from 1 to 4 km s^{-1} whilst the matrix velocity in Layer 2 is constant at 2.5 km s^{-1} giving velocity contrasts from low-to-high to high-to-low. The percentage anisotropy in Layer 2 varies from 0 up to 20 per cent. The open and closed squares mark the reflection coefficients for the shear waves polarized perpendicular and parallel to the cracks respectively at the top of the reservoir region in Fig. 9.

shear wave velocity in Layer 2 is 2.5 km s^{-1}. The curves were calculated using the standard reflection coefficient formula for an isotropic/isotropic interface:

$$reflection coefficient = (\rho_1 V_{S_1} - \rho_2 V_{S_2})/(\rho_1 V_{S_1} + \rho_2 V_{S_2}),$$

where ρ_1, ρ_2, and V_{S_1} and V_{S_2} are the densities and shear wave velocities in Layers 1 and 2, respectively. To account for the change in percentage anisotropy the velocity in Layer 2, V_{S_2} was varied. The 0 per cent anisotropy curve also represents the reflection coefficient curve for the shear wave polarized parallel to the cracks for each case assuming that the anisotropy is caused by thin cracks and that increasing the anisotropy does not greatly affect the velocities in the fast direction. If the upper layer was also anisotropic (with a constant background level of anisotropy) a similar approach could still be used but different velocities parallel and perpendicular to the cracks for Layer 1 would have to be used in the equation for reflection coefficients. The density in each layer was 2.2 g cm^{-3}. The density contrast affects the position of the curves shown in Fig. 10, but not their shape. A high-to-low density contrast will move the curves to the left, and a low-to-high density contrast to the right. Well-log data from a region will provide information about the density and velocity contrasts that can be expected from a given producing formation. Curves, similar to the ones shown in Fig. 10, could be plotted for a particular site to see whether there will be the necessary differences in reflection coefficients parallel and perpendicular to the fractures to be able to use this technique.

It can be seen from Fig. 10 that the absolute difference between the reflection coefficient curves for different percentage anisotropies does not vary significantly with velocity contrast. However, as the velocity contrast becomes small, near the centre of the graph, the values of the reflection coefficients decrease. This means that for small velocity contrast changes in anisotropy in the reflecting layer lead to large percentage differences between the amplitudes of the shear waves polarized parallel and perpendicular to the strike of the cracks. Conversely, for large velocity contrasts, changes in anisotropy lead to small percentage differences in the amplitudes of the shear waves polarized parallel to and perpendicular to the cracks. To be able to locate reservoirs which are only slightly more anisotropic than the surrounding rock mass, by looking for reflection amplitude discontinuities on the slow section (Mueller 1991), the velocity contrast at the rock interface with the layer containing the reservoir zone must be small. If the reservoir is highly anisotropic (heavily fractured), the anomalies should be visible even for large velocity contrasts. The exact details would depend on the particular velocity and density contrasts at the site under investigation.

As an example the reflection coefficients for the reflection from the top of Layer 3 (Fig. 9) are marked in Fig. 10. The solid square marks the reflection coefficient for the shear wave polarized parallel to the fractures and the open square marks the reflection coefficient of the shear wave polarized perpendicular to the fractures. From Fig. 10 it can be seen that there is a large difference between the reflection coefficient polarized parallel to and perpendicular to the cracks in the reservoir layer. This suggests that the reservoir would be visible as a reflection discontinuity on the slow reflection section (as is seen in Fig. 9) or by comparison of reflected amplitudes parallel to and perpendicular to the cracks. The use of graphs as in Fig. 10 provides an easy method for seeing if shear wave reflection amplitude methods are viable at a particular site.

4 DISCUSSION AND CONCLUSIONS

We have investigated the use of shear-wave amplitude variations with offset and vertical incidence reflection amplitude measurements in order to see if reservoir properties can be estimated when the layer thickness is too small for appreciable time delays to build up between the faster and slower split shear waves. Shear-wave AVOs are sensitive both to changes in percentage anisotropy and crack content, for thin cracks in the reflecting layer. The amplitude of the near-vertical reflected shear wave polarized perpendicular to the cracks varies with percentage anisotropy and the position of the zero point in the AVO curves changes. This suggests that the percentage anisotropy in a reflecting layer can be determined by analysis of shear-wave AVOs. The shear-wave AVO curves also change with variations in crack content for thin cracks, however such changes are only significant for wide offset data and the use of shear waves to examine crack content may be more suited to crosshole surveys.

Shear-wave amplitudes are difficult to measure if the acquistion plane is not parallel or perpendicular to the crack orientation at an isotropic/anisotropic interface due to the differences in reflection coefficients for SV- and SH-waves. Further distortions will occur if the upper layers are also anisotropic.

The greatest and most robust change in the shear-wave reflection coefficients for increasing reservoir anisotropy is for near-vertical incidence. Current methods for using this property to determine fracture density were reviewed. Any method which uses the change in polarization direction of a reflected shear wave is likely to lead to wrong conclusions in field data sets where the near-surface layers are also anisotropic. Such surface layers would mask the effects of reflections from an anisotropic layer. The comparison of reflected amplitudes of shear waves polarized parallel and perpendicular to the crack strike (or reflection continuity on the shear-wave section perpendicular to the fracture strike) may be an effective method to locate fractured reservoirs (Mueller 1991). A simple graphical approach has been suggested to determine whether the velocity and density contrasts in a particular area are suitable for such techniques.

ACKNOWLEDGMENTS

This work was supported by the Sponsors of the Edinburgh Anisotropy Project and the Natural Environment Research Council and is published with the approval of the Sponsors and of the Director of the British Geological Survey (NERC).

REFERENCES

Aki, K. & Richards, P. G., 1980. *Quantitative Seismology*, vol. 1, Freeman, San Francisco.

Alford, R. M., 1986. Shear-data in the presence of azimuthal anisotropy: Dilley, Texas, ***Expanded Abstracts, 56th Ann. Znt. SEG Mtg, 1986, Houston,*** pp. 476-479.

Becker, D. F., Bishop, G. L., Clayton, K. N., Peterson, D. N., Rendleman, C. A. & Shah, P. M., 1990. Shear-wave anisotropy at Marcelina Creek, ***Abstract, SEG Workshop: Vector Field Seismology Update, San Francisco,*** p. 19.

Booth, D. C. & Crampin, S., 1983. The anisotropic reflectivity technique: theory, ***Geophys. J. R. astr. Soc., 72, 755-766.***

Booth, D. C. & Crampin, S., 1985. Shear-wave polarization on a curved wavefront at an isotropic free surface, ***Geophys. J. R. astr. Soc., 83,*** 31-45.

Bush, I., 1990. Modelling shear-wave anisotropy in the Paris Basin, ***PhD dissertation,*** University of Edinburgh.

Corbett, K., Friedman, F. & Spang, J., 1987. Fracture development and mechanical stratigraphy of Austin Chalk, Texas, ***AAPG Bull., 71, 17-28.***

Crampin, S., 1970. The dispersion of surface waves in multilayered anisotropic media, ***Geophys. J. R. astr. Soc., 21, 387-402.***

Crampin, S., 1984. Effective elastic-constants for wave propagation through cracked solids, ***Geophys. J. R. astr. Soc., 76,*** 135-145.

Crampin, S., 1987. Geological and industrial implications of extensive-dilatancy anisotropy, ***Nature, 328,*** 491-496.

Crampin, S., Lynn, H. B. & Booth, D. C., 1989. Shear-wave VSPs: a powerful new tool for fracture and reservoir description, *J. pet. Technn., 5, 283-288.*

Fuchs, K. & Miiller, G., 1971. Computation of synthetic seismograms with the reflectivity method and comparison with observations, ***Geophys. J. R. astr. Soc., 23,*** 417-433.

Gilbert, F. & Backus, G. E., 1966. Propagator matrices in elastic wave and vibration problems, ***Geophysics, 31, 326-332.***

Hudson, J. A., 1980. Overall properties of a cracked solid, ***Math. Proc. Camb. phil. Soc.,*** **88,** 371-384.

Hudson, J. A., 1981. Wave speeds and attenuation of elastic waves in material containing cracks, ***Geophys. J. R. astr. Soc.***, **64,** 133-150.

Kaye, G. W. C. & Laby, T. H., 1986. ***Tables of Physical and Chemical Constants,*** Longman, London.

King, M. S., 1966. Wave velocities in rocks as a function of changes in overburden pressure and pore fluid saturants, ***Geophysics,*** **31,** 50–73.

Liu, E., Crampin, S. & Yardley, G. S., 1990. Polarizations of reflected shear waves, ***Geophys. Res. Lett.,*** 17, 1137-1140.

McCamy, K., Meyer, R. P. & Smith, T. J., 1962. Generally applicable solutions of Zoeppritz's amplitude equations, ***Bull. seism. Soc. Am., 52, 923-955.***

Mueller, M. C., 1991. Prediction of lateral variability in fracture intensity using multicomponent shear wave surface seismic as a precursor to horizontal drilling in the Austin Chalk, ***Geophys. J. Znt.,*** **107,** this issue.

Ostrander, W. J., 1984. Plane-wave reflection coefficients for gas sands at nonnormal angles of incidence, ***Geophysics, 49,*** 1637-1648.

Spencer, T. W. & Chi, H. C., 1990. Thin layer fracture density, ***Expanded Abstracts, 60th Ann. Znt. SEG Mtg, 1990, San Francisco,*** vol. 2, pp. 1386-1387.

Taylor, D. B., 1990. ***ANZSEZS Manual,*** version 4.5, Applied Geophysical Software, Houston.

Thomsen, L., 1988. Reflection seismology over azimuthally anisotropic media, ***Geophysics, 53,*** 304-313.

Wang, Z. & Nur, A., 1988. Effect of temperature on wave velocities in sands and sandstones with heavy hydrocarbons, ***SPE Reservoir Eng., 3, 158-164.***

Wang, Z. & Nur, A., 1990. Wave velocities in hydrocarbon-saturated rocks: Experimental results, ***Geophysics, 55,*** 723-733.

Ziolkowski, A., 1991. Why don't we measure seismic signatures?, ***Geophysics, 56,*** 120-201.